J Electr Eng Technol.2017; 12(2): 726-737
https://doi.org/10.5370/JEET.2017.12.2.726

ISSN(Print) 1975-0102
ISSN(Online) 2093-7423

Optimal Power Control Strategy for Wind Farm with Energy Storage System

Cong-Long Nguyen* **and Hong-Hee Lee†**

Abstract – The use of energy storage systems (ESSs) has become a feasible solution to solve the wind power intermittency issue. However, the use of ESSs increases the system cost significantly. In this paper, an optimal power flow control scheme to minimize the ESS capacity is proposed by using the zero-phase delay low-pass filter which can eliminate the phase delay between the dispatch power and the wind power. In addition, the filter time constant is optimized at the beginning of each dispatching interval to ensure the fluctuation mitigation requirement imposed by the grid code with a minimal ESS capacity. And also, a short-term power dispatch control algorithm is developed suitable for the proposed power dispatch based on the zero-phase delay low-pass filter with the predetermined ESS capacity. In order to verify the effectiveness of the proposed power management approach, case studies are carried out by using a 3-MW wind turbine with real wind speed data measured on Jeju Island.

Keywords: Energy storage systems (ESSs), Hybrid wind and energy storage system, Power flow control, Zero-phase low-pass filter, Fluctuation mitigation requirement (FMR)

1. Introduction

The use of energy storage systems (ESSs) has become a feasible solution to mitigate the wind power fluctuation problem [1], [2]. Although wind power is a clean and infinite source to solve the current global energy problems such as the exhaustion of fossil fuels and the impact of environmental pollution, the wind power fluctuation problem negatively impacts on the quality, stability, and reliability of the power grid [3]. In order to mitigate this wind power fluctuation, ESSs have been actively utilized. Due to the rapid development of ESSs such as battery energy storage systems (BESSs), super-conducting magnetic energy storage (SMES), electric double-layer capacitors (EDLC), and flywheels, these ESSs can feasibly handle the wind power fluctuation issue [4].

Although the hybrid wind and energy storage system is able to supply stable power to the grid, the cost of ESS installation adds an additional expense to the system [5]. In [6], the storage cost per kWh was analyzed to show that the ESS increases the retail electricity price by three times. The significant additional cost due to the ESSs requires optimization of the hybrid system operation to minimize the ESS capacity. Optimization of the hybrid system operation means optimizing the power flow of the dispatch power and the ESS power [7].

So far, three popular power flow control methods have been presented to manage the hybrid system operation. The first method is based on the low-pass filter (LPF), where the dispatch power is determined by passing the wind power through the LPF [8]. The second method is the constant power dispatch, where the dispatch power is the average value of the wind power in each hour [9]. The third method named the min-max dispatching strategy was introduced in [10], where the dispatch power is assigned with either the minimum or maximum wind power in each dispatching interval. Among these three power flow control methods, the LPF based method is usually used because it does not require the wind power forecast and the required ESS capacity is smaller than those of the others [11].

In the LPF-based power flow control method, both infinite and finite impulse response types have been applied to mitigate the wind power fluctuation. In the infinite impulse response LPF, the first-order filter is usually adopted [12]. However, the phase delay in the pass-band of the filter requires a high capacity ESS. To address this problem, a power dispatching method based on the zero-phase LPF was firstly introduced in [13]. However, in this method, the time constant of the filter is not optimized during the system operation, so that the required ESS capacity is still high. Furthermore, the hybrid system operation in short-term was not taken into account.

In this paper, an optimal power flow control strategy is developed by using a zero-phase delay LPF with an optimal time constant, which was succinctly introduced in [14]. The time constant of the filter that can minimize the ESS capacity is derived at the beginning of each dispatching interval from the relationship between the time constant and the ESS capacity. In order to determine the

† Corresponding Author: School of Electrical Engineering, University of Ulsan, Korea. (hhlee@mail.ulsan.ac.kr)
* Dept. of Electrical Engineering, École de technologie supérieure, University of Quebec, Quebec, Canada. (conglongbk@gmail.com)
Received: March 18, 2016; Accepted: November 7, 2016

optimal time constant of the filter, a searching flowchart is developed to ensure that the hybrid system dispatches a stable power to the grid with the minimal ESS capacity. Moreover, a short-term power dispatch control algorithm is presented to manage the power flow of the hybrid system in short-term. In the proposed short-term power dispatch control algorithm, a power control signal is added to the dispatch power command to regulate the power and state of charge (SOC) of the ESS to ensure them within the predefined safe ranges. The effectiveness of the proposed optimal control strategy is verified through a 3-MW wind farm with real wind data measured on Jeju Island.

2. Wind Power Fluctuation

In order to evaluate the dispatchability of the wind power system, the fluctuation of the wind power should be taken into account. It is well known that the output power of a wind turbine (WT), $P_w(t)$, is a cubic function of wind speed, $v(t)$, as follows:

$$P_w(t) = \frac{1}{2} C_p(\lambda, \beta) \rho \pi R^2 v^3(t). \quad (1)$$

where ρ is the air density and R is the radius of the WT. And, $C_p(\lambda, \beta)$ is the power coefficient, which is a function of the tip-speed ratio, λ, and the pitch angle, β [15]. Because the wind speed depends on the natural and meteorological conditions, the WT output power essentially fluctuates. Fig. 1(a) shows the power response during one month of a 3-MW WT in Jeju Island. It is shown that the wind power can vary from the WT power rating to zero for a short interval. In order to study the fluctuation level of the power $P_w(t)$, the power fluctuation in the $\kappa-$min time window is defined as:

$$\Delta F_{\mathrm{w}}^{\kappa}(t) = \frac{\underset{t-\kappa\le\tau\le t}{\mathrm{MAX}}\{P_{\mathrm{w}}(\tau)\} - \underset{t-\kappa\le\tau\le t}{\mathrm{MIN}}\{P_{\mathrm{w}}(\tau)\}}{P_{\mathrm{WTR}}}, \quad (2)$$

where P_{WTR} is the WT power rating. In Fig. 1(b), the wind power fluctuation in the 1-min time window, i.e. $\Delta F_w^1(t)$, is plotted. It can be seen that in a 1-min interval, the wind power can vary up to 35% of the WT power rating. With such a high wind power fluctuation, the high penetration level of the wind farm into the grid would seriously impact the power quality and reliability of the electric grid [16]. Due to these negative impacts on the wind power fluctuation, the transmission system operator of each country has issued a specific grid code to define the technical requirements for the connection of wind farms [17]. One of the most important aspects in the grid code is the active power control which regulates the maximum fluctuation of the dispatch power during the wind farm startup and shutdown, or the wind speed variation.

Similar to the definition of wind power fluctuation, the dispatch power fluctuation level is defined as follows:

$$\Delta F_{\mathrm{d}}^{\kappa}(t) = \frac{\underset{t-\kappa\le\tau\le t}{\mathrm{MAX}}\{P_{\mathrm{d}}(\tau)\} - \underset{t-\kappa\le\tau\le t}{\mathrm{MIN}}\{P_{\mathrm{d}}(\tau)\}}{P_{\mathrm{WTR}}}, \quad (3)$$

where $P_{\mathrm{d}}(t)$ is the dispatch power onto the grid. Usually, the grid code specifies that the dispatch power fluctuation in the $\kappa-$min time window must not exceed the upper limit as

$$\Delta F_{\mathrm{d}}^{\kappa}(t) \le \gamma_{\kappa-\min}, \quad (4)$$

where $\gamma_{\kappa-\min}$ is the maximum fluctuation of the dispatch power, which is the fluctuation mitigation requirement (FMR) imposed by the grid codes. Based on the FMR in the common grid codes [17], it is clear that the wind power that varies at such a high level as shown in Fig. 1 cannot be dispatched to the grid.

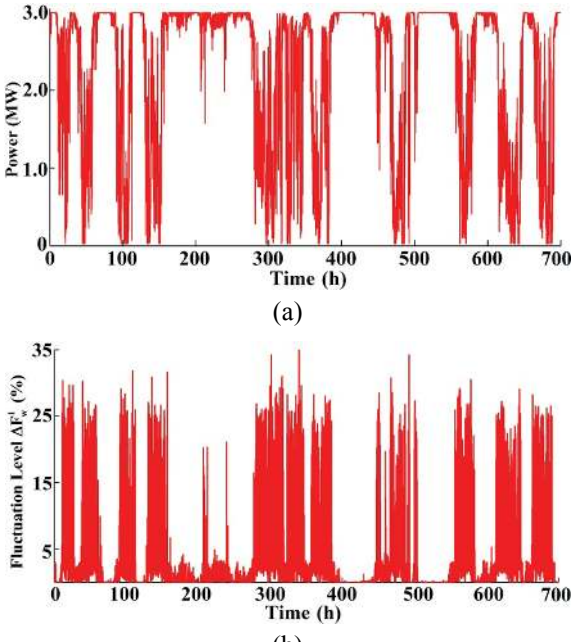

Fig. 1. Wind power variation: (a) Output power of 3-MW WT in one month; (b) Wind power fluctuation level in 1-min time window.

3. Hybrid Wind and Energy Storage System

In order to comply with the grid code requirement, the wind power fluctuation must be mitigated sufficiently to ensure that the dispatch power has a fluctuation lower than the $\gamma_{\kappa\text{-min}}$ limit. Using the ESSs in the wind power application is a feasible solution to mitigate the wind power fluctuation. Unlike the peak shaving or load leveling application where the ESS plays as a distributed generation

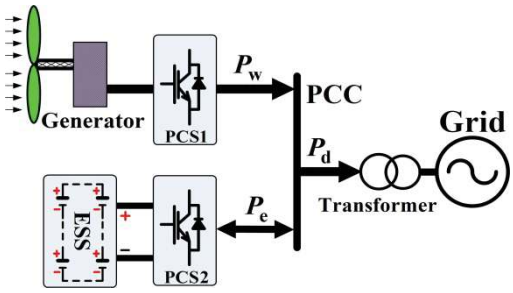

Fig. 2. Common configuration of hybrid wind and energy storage system.

to meet the load demand of the grid [18]-[19], the ESS in wind power application is used to compensate the wind power fluctuation as an energy buffer. Fig. 2 illustrates a common configuration of energy storage system in wind power, where both the WT generator and the ESS are connected to the grid at the point of common coupling (PCC) through their power converter systems PCS1 and PCS2. While the output of the generator $P_w(t)$ and the dispatch power $P_d(t)$ are always positive, the ESS output power $P_e(t)$ can be either positive or negative powers corresponding to the charge or discharge states of the storage device. If the power losses in the PCSs are neglected, the ESS power, $P_e(t)$, can be defined as

$$P_e(t) = P_w(t) - P_d(t). \quad (5)$$

3.1 Power and energy ratings of ESS

The minimum requirement of ESS capacity, which is normally specified in terms of energy rating E_e^{rat} and power rating P_e^{rat}, is determined based on the power dispatch and the WT output power profiles [10]. Considering that the system is operating in a time duration T, the ESS power rating is defined as

$$P_e^{rat} = \underset{0\le t\le T}{\text{MAX}} |P_e(t)| = \underset{0\le t\le T}{\text{MAX}} |P_w(t) - P_d(t)|. \quad (6)$$

The integrated ESS power with respect to time yields the net energy injected into or drawn from the storage up to time t:

$$E_e(t) = \int_0^t P_e(\tau)d\tau = \int_0^t [P_w(\tau) - P_d(\tau)]d\tau. \quad (7)$$

Similar to the power rating, the energy rating is the maximal energy value being stored or released by the ESS during the system operation time T, and is defined as follows:

$$E_e^{rat} = \frac{\underset{0\le t\le T}{\text{MAX}}[E_e(t)] - \underset{0\le t\le T}{\text{MIN}}[E_e(t)]}{\text{DOD}}, \quad (8)$$

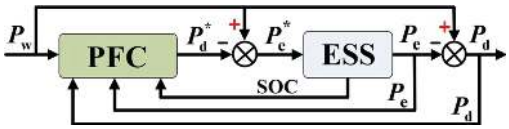

Fig. 3. Power flow control scheme for the hybrid wind and energy storage system.

where DOD denotes the depth of discharge of the ESS. Because a high DOD causes significant degradation of the storage lifetime, a limitation of DOD needs to be set during discharging; the maximum DOD is usually set at 80%.

3.2 Power flow control of hybrid wind and energy storage system

Fig. 3 illustrates the general PFC scheme for the hybrid wind and energy storage system, where the dispatch power command, P_d^*, is defined based on the wind power, the ESS power, the dispatch power, and the SOC of ESS [20]. Afterwards, the ESS power command is obtained by subtracting the dispatch power command from the wind power. Fundamentally, the power flow control scheme must perform three requirements: 1) the dispatch power is optimized to minimize the ESS capacity under the given FMR condition; 2) the output power of ESS should not exceed the ESS power rating; and 3) the SOC of the ESS must be within a safe range. The first requirement is usually taken into account during the design and planning of the hybrid system [21]. At this stage, the long-term wind power profile in history is collected to evaluate the availability and the characteristic of the wind power at the wind farm. Meanwhile, the second and third requirements are considered in the short-term power dispatching control of the hybrid system in the real time [22]. In this paper, we develop an optimal power flow control strategy for the hybrid system by considering all such three requirements.

4. Low-pass filter Based Power Flow Control

Even though a zero-phase LPF has been introduced in order to remove the inherent phase delay, the required ESS capacity cannot be minimized sufficiently, while the output power and SOC of ESS cannot be guaranteed within predefined safe ranges because the time constant of the zero-phase LPF is not optimized. In order to solve these problems, the time constant T_c of the zero-phase LPF is optimized by considering the wind power $P_w(t)$, the dispatch power $P_d(t)$, the ESS power $P_e(t)$, and the SOC of ESS as shown in Fig. 4. Based on the optimal T_c and the wind power information, we determine the filtered power $P_f(t)$ which is one part of the dispatch power command. In addition, the proposed optimal power flow control scheme regulates the SOC and the power of the ESS by adding a power control $P_c(t)$ to the filtered power to generate the power command for the PCS2. The commands

of the dispatch power and the ESS power are defined as

$$P_{\mathrm{d}}^{*}(t) = P_{\mathrm{f}}(t) + P_{\mathrm{c}}(t) \tag{9}$$

$$P_{\mathrm{e}}^{*}(t) = P_{\mathrm{w}}(t) - \left[P_{\mathrm{f}}(t) + P_{\mathrm{c}}(t)\right] \tag{10}$$

PCS2 regulates the ESS power to follow its command, $P_{\mathrm{e}}^{*}(t)$, and in the steady state, the following relationship is obtained during the operation of the hybrid system:

$$P_{\mathrm{d}}(t) = P_{\mathrm{f}}(t) + P_{\mathrm{c}}(t) \tag{11}$$

$$P_{\mathrm{e}}(t) = P_{\mathrm{w}}(t) - \left[P_{\mathrm{f}}(t) + P_{\mathrm{c}}(t)\right] \tag{12}$$

In this section, the first role of the power flow control scheme, which is to determine the optimal time constant of the zero-phase LPF, is presented to minimize the required ESS capacity. This role is usually taken into account during the design and planning of the hybrid system. Therefore, the SOC of ESS and the power control $P_{\mathrm{c}}(t)$ are neglected in this section. In other words, the filtered power $P_{\mathrm{f}}(t)$ refers to the dispatch power $P_{\mathrm{d}}(t)$.

4.1 Design of zero phase low-pass filter

As shown in Fig. 4, the power flow of the hybrid system is determined by passing the wind power through the zero-phase LPF. Because the zero-phase LPF has no phase delay in the pass-band, the wind power can be smoothened to obtain a reduced required ESS capacity. To effectively design the zero-phase LPF with a reduced number of coefficients, a symmetrical forward-reverse digital finite impulse response filter is applied, which is defined as follows

$$H(z) = \alpha_0 + \sum_{k=1}^{\mathrm{K}} \alpha_k (z^{k} + z^{-k}) . \tag{13}$$

Its frequency response is derived as

$$H(e^{j\omega T_s}) = \alpha_0 + 2\sum_{k=1}^{\mathrm{K}} \alpha_k \cos(k\omega T_s) , \tag{14}$$

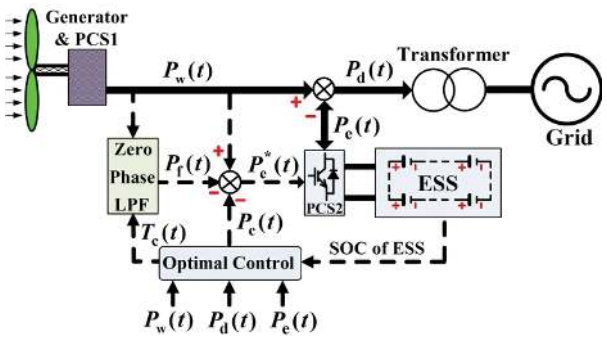

Fig. 4. Proposed power flow control scheme for hybrid wind and energy storage system.

where K is the length of the filter coefficient and T_{s} is the sampling time. The frequency response is absolutely real when all coefficients α_k are real, which leads to a zero-delay time response for the filter. In other words, the phase delay can be canceled out by adopting the zero-phase LPF. The filter coefficients α_k are dependent on the filter time constant, T_{c}. The array (h) containing the first N values of the impulse response of the first-order LPF is defined as following:

$$h = \left[h_0 \ \ldots \ h_k \ \ldots \ h_N\right], \tag{15}$$

where

$$h_k = \frac{1}{T_c} e^{\frac{-k}{T_c}} ; \quad k = 0,\ 1,\ \ldots ,\ N . \tag{16}$$

Then, h is convolved with itself and normalized to yield the coefficients of zero-phase LPF as (17) and (18).

$$\tilde{\alpha}_k = \sum_{n=k}^{N} h_n h_{n-k} ; \quad k = 0,\ 1,\ \ldots ,\ N . \tag{17}$$

$$\alpha_k = \frac{\tilde{\alpha}_k}{\tilde{\alpha}_0 + 2\sum_{n=1}^{N} \tilde{\alpha}_n} ; \quad k = 0,\ 1,\ \ldots ,\ N . \tag{18}$$

The dispatch power (i.e. the filtered power) and ESS power are computed as

$$P_{\mathrm{d}}(t) = P_{\mathrm{f}}(t) = \alpha_0 P_{\mathrm{w}}(t) + \sum_{k=1}^{\mathrm{K}} \alpha_k \left[P_{\mathrm{w}}(t - kT_{\mathrm{s}}) + P_{\mathrm{w}}(t + kT_{\mathrm{s}})\right] \tag{19}$$

$$P_{\mathrm{e}}(t) = \left[1 - \alpha_0\right] P_{\mathrm{w}}(t) - \sum_{k=1}^{\mathrm{K}} \alpha_k \left[P_{\mathrm{w}}(t - kT_{\mathrm{s}}) + P_{\mathrm{w}}(t + kT_{\mathrm{s}})\right] \tag{20}$$

4.2 Optimization of the filter time constant

The Eqs. (19) and (20) represent the model of the proposed power flow control scheme based on the zero-phase LPF. It can be seen that the filter time constant determines the ESS power and the dispatch power. To make the wind conversion system dispatchable, the dispatch power of the hybrid system must satisfy the FMR imposed by the grid code. Therefore, the filter time constant should be determined optimally to ensure the dispatch power meets the FMR with the minimal required ESS capacity. In order to find the optimal filter time constant, the relationships among the filter time constant, the FMR, and the required ESS capacity need to be firstly evaluated.

In Fig. 5, the relationships among the filter time constant, the FMR, and the required ESS capacity are shown by

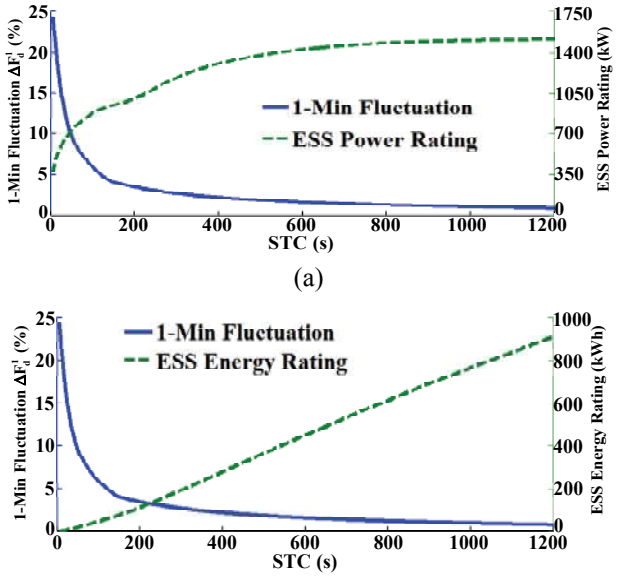

Fig. 5. Filter time constant versus ESS capacity and fluctuation level of dispatch power: (a) 1-min fluctuation of dispatch power and ESS power rating; (b) 1-min fluctuation of dispatch power and ESS energy rating.

evaluating a 3-MW WT system during one month. Based on Fig. 5, a critical remark is noted here:

Remark I: As the filter time constant increases, the obtained smoothing power dispatch level also increases, but a higher ESS capacity is required.

From Remark I, the definition of the optimal filter time constant is:

Definition I: The optimal filter time constant is the smallest value that leads the dispatch power to meet the FMR.

Finally, a searching method to determine the optimal filter time constant is obtained as depicted in Fig. 6. At the beginning of each hour, the proposed searching process is executed to determine the optimal filter time constant. Initially, the previous value of filter time constant is used to determine the power flow of the system in (19) and (20). If the dispatch power does not satisfy the FMR defined in (4), the filter time constant value in the previous dispatching interval hour may be too small; the filter time constant should then be increased until the dispatch power satisfies the FMR. Otherwise, when the dispatch power determined by the filter time constant in the previous dispatching hour satisfies the FMR, the filter time constant may be too large; we should thus reduce the filter time constant until the FMR cannot be obtained. Because the searching process initializes the filter time constant in the previous dispatching hour, the computation time is relatively short. In addition, the proposed searching method is essentially a linear search. Therefore, the proposed searching flowchart

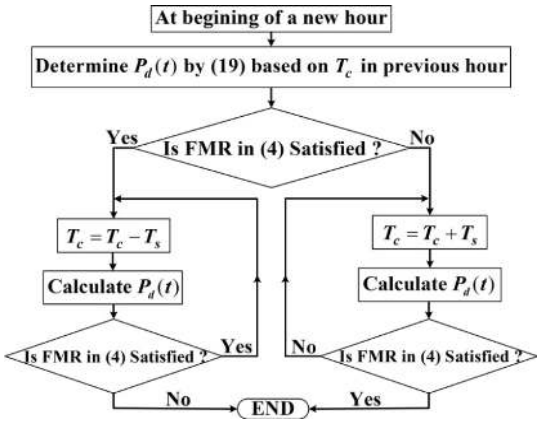

Fig. 6. Proposed flowchart used to search the optimal filter time constant.

is easy to implement in a real operation.

5. Short-term Power Dispatch Control

The short-term power dispatch control means that the power flow of the hybrid system including the dispatch power and the ESS power is controlled to obtain the FMR imposed by the grid code, and to ensure the SOC and power of ESS are within the predefined safe ranges. In order to meet these requirements, an additional power control signal $P_c(t)$ is added to the filtered wind power to regulate the ESS power as shown in Fig. 4. Furthermore, because the wind power information in the future is not given during the short-term power dispatch control, the wind power must be forecasted to control the power flow of the hybrid system. In this paper, the error between the forecasted and the real wind power is described in the form of a normal distribution with a constant mean and standard deviation [23].

In order to determine $P_c(t)$, an optimal control algorithm is proposed based on the information of the dispatch power, the wind power, the SOC, and the power of ESS. The control objective function is defined as

$$f\left(P_c(t)\right) = k_p \left|P_c(t)\right| + k_s \left| SOC(t) - \frac{SOC_U + SOC_L}{2} \right|, \quad (21)$$

where k_p and k_s are the control coefficients. Meanwhile, SOC_U and SOC_L denote the upper and lower limits of SOC. In the control objective function, the first term is the power control signal used to stabilize the system operation, while the second term aims to regulate the SOC to be the middle point of the safe range. So, obtaining the optimal value of $P_c(t)$ implies that the control objective function is minimal when that value is added into the dispatch power command. In other words, the process used to search the optimal value of $P_c(t)$ can be described as follows:

$$\min_{P_c(t)\in[-P_e^{rat},\,P_e^{rat}]} f = \min\left\{k_p\left|P_c(t)\right| + k_s\left|SOC(t) - \frac{SOC_U + SOC_L}{2}\right|\right\} \tag{22}$$

with the following two constraints:

1) The ESS power must be within the power rating as

$$\left|P_e(t)\right| \le P_e^{rat} \tag{23}$$

2) The fluctuation of the dispatch power must satisfy the FMR as

$$\Delta F_d^{\kappa}(t) = \frac{\underset{t-\kappa\le\tau\le t}{\mathrm{MAX}}\left\{P_f(\tau)+P_c(\tau)\right\} - \underset{t-\kappa\le\tau\le t}{\mathrm{MIN}}\left\{P_f(\tau)+P_c(\tau)\right\}}{P_{WTR}} \le \gamma_{\kappa-\min} \tag{24}$$

In the control objective function, the coefficients k_p and k_s take a critical role to regulate the SOC of ESS. The principle to define the optimal value of k_p and k_s is that when the SOC reaches close to the upper or lower limit, k_s should be increased and k_p should be decreased to ensure the SOC is at the middle point of the safe SOC range. The following equations describe the proposed principle of determining k_p and k_s:

$$k_p = \begin{cases} k_p^{\min} & \text{if } SOC \le 0.3 \\ \dfrac{k_p^{\max}-k_p^{\min}}{0.3}SOC + \dfrac{0.6k_p^{\min}-0.3k_p^{\max}}{0.3} & \text{if } 0.3 \le SOC \le 0.6 \\ \dfrac{k_p^{\min}-k_p^{\max}}{0.3}SOC + \dfrac{0.9k_p^{\max}-0.6k_p^{\min}}{0.3} & \text{if } 0.6 \le SOC \le 0.9 \\ k_p^{\min} & \text{if } SOC \ge 0.9 \end{cases} \tag{25}$$

$$k_s = \begin{cases} k_s^{\max} & \text{if } SOC \le 0.3 \\ \dfrac{k_s^{\min}-k_s^{\max}}{0.2}SOC + \dfrac{0.5k_s^{\max}-0.3k_s^{\min}}{0.2} & \text{if } 0.3 < SOC \le 0.5 \\ k_s^{\min} & \text{if } 0.5 < SOC \le 0.7 \\ \dfrac{k_s^{\max}-k_s^{\min}}{0.2}SOC + \dfrac{0.9k_s^{\min}-0.7k_s^{\max}}{0.2} & \text{if } 0.7 < SOC < 0.9 \\ k_s^{\max} & \text{if } SOC \ge 0.9 \end{cases} \tag{26}$$

where $k_s^{\max}$ and $k_s^{\min}$ are the maximum and minimum value of the coefficient k_s, respectively, whereas $k_p^{\max}$ and $k_p^{\min}$ are the maximum and minimum value of the coefficient k_p, respectively, and they are defined as following: $k_p^{\max} = 1/P_e^{rat}$, $k_p^{\min} = 0.25/P_e^{rat}$, $k_s^{\max} = 1$, and $k_s^{\min} = 0.25$. Fig. 7 and Fig. 8 illustrate the value of k_p and k_s with respect to the SOC, respectively. When the ESS reaches close to the deep discharge status (i.e. $SOC \le 0.3$), k_s is set to be the maximum and k_p is set to be the minimum. This means the minimal allowable value of $P_c(t)$ can be added to the power dispatch command, so the SOC can be increased to prevent the ESS from being the deep discharge status. In the case where the SOC is a normal condition but is still close to the deep discharge status (i.e. $0.3 \le SOC < 0.5$), k_s is linearly decreased and k_p is linearly increased to define the suitable value of $P_c(t)$. When the SOC is around the middle point (i.e. $0.5 \le SOC \le 0.7$), $P_c(t)$ does not need to be added to the dispatch power command. Therefore, k_s is set to be the minimum in this case, as shown in Fig. 8. When the ESS is close to the full charge (i.e. $SOC \ge 0.9$), k_s is set to be the maximum and k_p is set to be the minimum. As a result, the maximal allowable value of $P_c(t)$ is added to the power dispatch command to prevent the ESS from being the full charge.

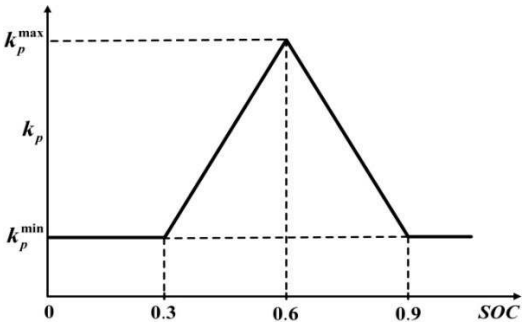

Fig. 7. Coefficient k_p with respect to the SOC.

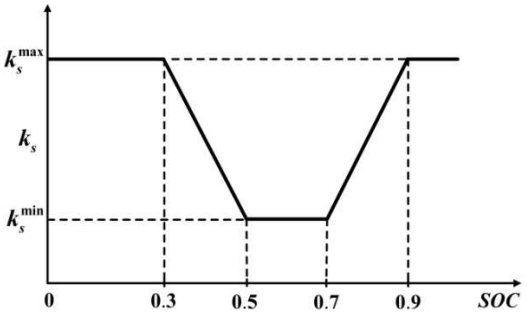

Fig. 8. Coefficient k_s with respect to the SOC.

To search the optimal value of $P_c(t)$, we can use the optimal search methods such as the particle swarm optimization approach [24] and the linear search method [25] to implement the search process described in (22)-(24). Because of its simple implementation feature, the linear search method is used to search the optimal value of $P_c(t)$, as shown in Fig. 9. Initially, the search variables P_c^s and $f_{\min}$ are set as zero and infinity, respectively. The coefficients k_p and k_s are then defined from the SOC of ESS as shown in Figs. 7 and 8, respectively. When the SOC is lower than 0.6, which means that the ESS has low energy, we should reduce the dispatch power to charge the ESS. Therefore, the search variable P_c^s is reduced step by

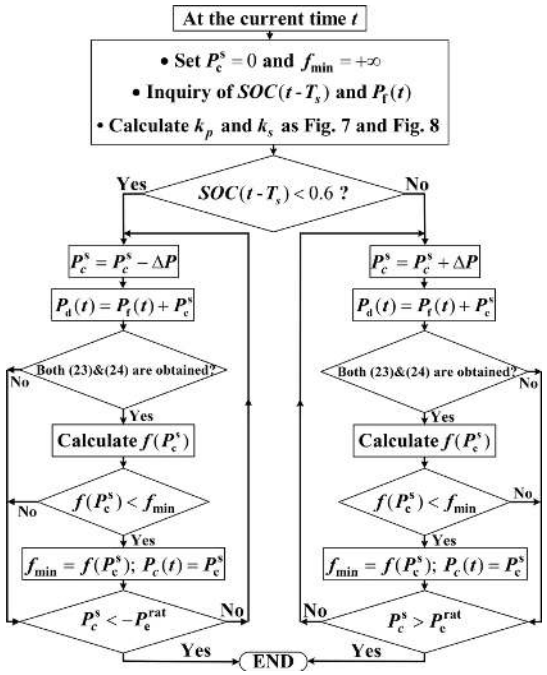

Fig. 9. Proposed flowchart used to search the optimal value of power control $P_c(t)$.

step as shown in the left part of Fig. 9. On the contrary, the search variable of the $P_c(t)$ is increased step by step when the SOC is higher than 0.6. The search target is to determine the P_c^s where the objective function f is minimal, which is designated as the optimal value of the power control signal $P_c(t)$.

6. Numerical Examples

In order to evaluate the effectiveness of the proposed optimal power control strategy, several simulations are carried out using the MATLAB software. For the assessment, a 3-MW WT is selected [26], and the real wind speed on Jeju Island in 2013 is measured with 10-s sampling (i.e. $T_S = 10$ s and $P_{WTR} = 3$ MW). We assume that the FMR is defined as $\gamma_{1-min} = 1\,\%$, which means the fluctuation of the dispatch power in 1-min must be maintained below 1% of the WT power rating. During the short-term power dispatch, the upper and lower limits of SOC are 0.2 and 1.0, respectively. This means that $SOC_L = 0.2$, $SOC_U = 1.0$, and DOD=0.8.

6.1 Optimization of ESS capacity

While determining the optimal ESS capacity, the SOC of ESS is neglected, and the power control signal $P_c(t)$ is set as zero; the filtered power $P_f(t)$ is the dispatch power $P_d(t)$. In Fig. 10, the performance of the proposed power control strategy is shown to determine the optimal ESS capacity, where the wind power data is measured in one day. We can

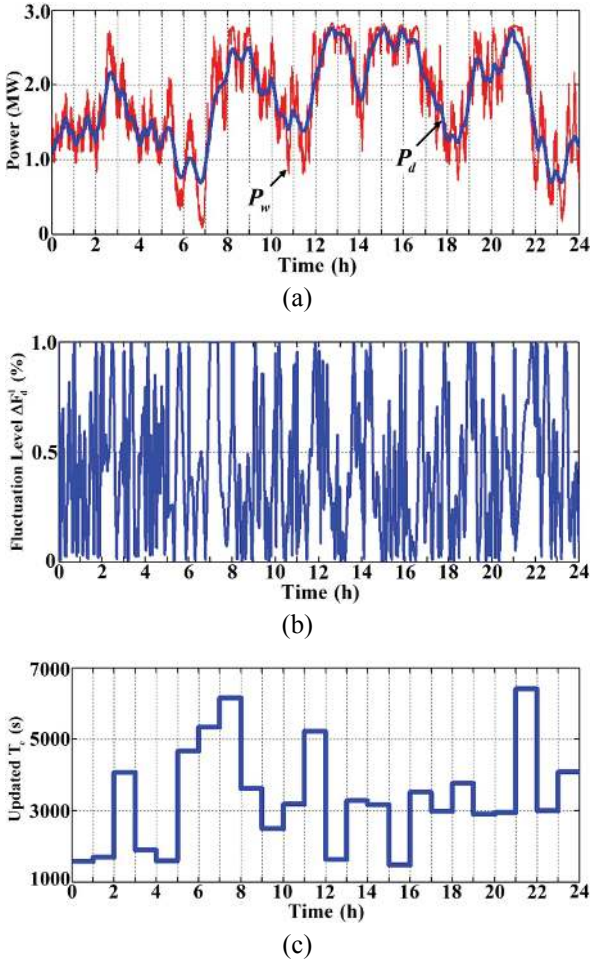

Fig. 10. Performance of the proposed optimal control scheme: (a) Dispatch power and wind power; (b) Fluctuation level of dispatch power in 1-min; (c) Filter time constant.

see that the fluctuation of the dispatch power is always maintained below 1% to satisfy the FMR as shown in Fig. 10(b). In order to obtain the FMR with the minimal ESS capacity, the time constant of the zero-phase LPF is optimized at the beginning of each hour. The time constant values are updated and shown in Fig 10(c). In the intervals when the wind power is highly fluctuated, the time constant should be high to sufficiently mitigate the wind power fluctuation. The maximum time constant is 6500 seconds required in the time intervals of 7:00-8:00 and 21:00-22:00 when the wind power fluctuates from zero up to the WT power rating in a short period of time. Notably, if the conventional method is applied, we need to set the time constant higher than 6500 seconds to ensure that the dispatch power obtains the FMR. This means the conventional method requires a higher ESS capacity than the proposed method.

The proposed method is compared with the conventional LPF method [12] and the conventional zero-phase low-pass filter (ZLF) method [13] in order to verify its effectiveness,

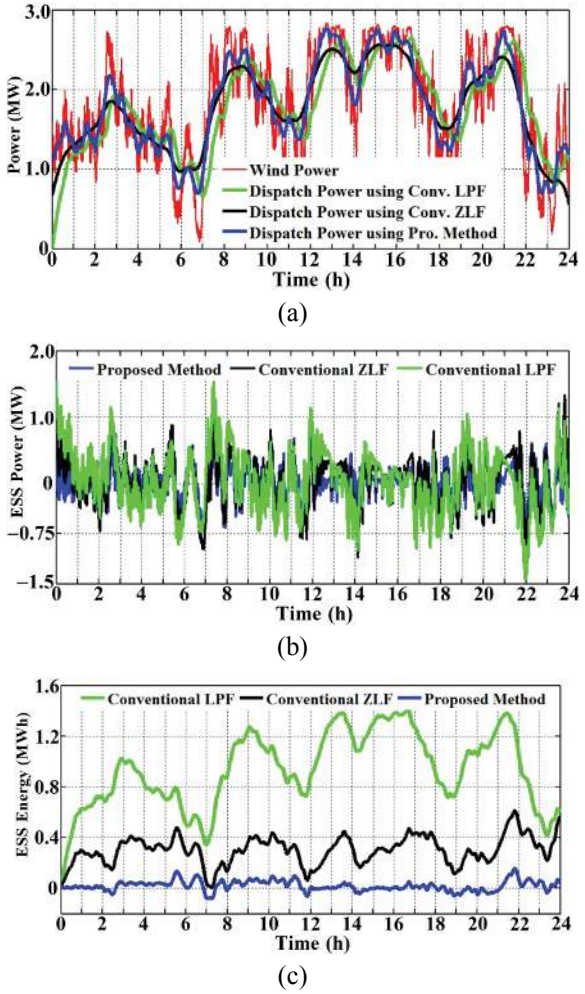

Fig. 11. Comparison of the conventional LPF method, the conventional ZLF method, and the proposed method: (a) Dispatch power and wind power; (b) ESS power response; (c) ESS energy response.

while the performances of the hybrid system using each control method are shown in Fig. 11. As expected, because the methods based on the zero-phase LPF can remove the phase delay between the dispatch power and wind power, the ESS power and ESS energy are reduced significantly as shown in Figs. 11(b) and 11(c). Compared with the conventional zero-phase LPF method, the proposed method can minimize the required ESS power and energy due to the optimal time constant of the zero-phase LPF in each hour. Based on Figs. 11(b) and 11(c) and the definition of the required ESS capacity as in (6) and (8), the required ESS power and energy rating is 1.6MW/1.8MWh with the conventional LPF method, 1.3MW/0.8MWh with the conventional zero-phase LPF, and 0.9MW/0.35MWh with the proposed method. Therefore, we can say that the proposed method can reduce the required ESS capacity significantly compared with the conventional methods.

In Fig. 12, we summarize the required ESS capacity in each of the three control methods respective of the four

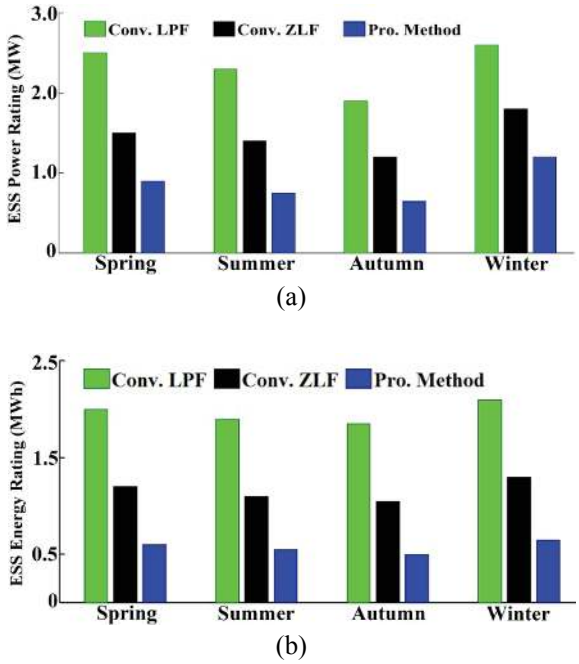

Fig. 12. Comparison of the required ESS capacity in the conventional LPF method, the conventional ZLF method, and the proposed method with respect to the four seasons: (a) ESS power rating; (b) ESS energy rating.

seasons of the year. Because the wind power in the winter season fluctuates more than in the other seasons, the required ESS capacity in winter is highest for all of the three methods. Therefore, the required ESS capacity is defined from the winter season; the required ESS capacity is 2.6MW/2.1MWh with the conventional LPF method, 1.8MW/1.3MWh with the conventional zero-phase LPF method, and 1.2MW/0.65MWh with the proposed method. These results demonstrate that the proposed control method can reduce significantly the required ESS capacity.

6.2 Short-term power dispatch control

During the short-term power dispatch control, the wind power in the future is not given exactly but is forecasted approximately to determine the power flow of the system. In this investigation, the error between the actual and the forecasted wind power is described in the form of a normal distribution with a mean of 0.05 and a standard deviation of 0.03. Fig. 13 shows the actual and the forecasted wind power from 10:00 to 11:00 in one day. Because a significant error occurs between the actual and the forecasted wind power, the control algorithm should consider this error to ensure the power and SOC of ESS are within the predefined safe ranges during the short-term power dispatch.

Based on Fig. 12, the ESS with 1.2 MW of the power rating and 0.65 MWh of the energy rating are installed to

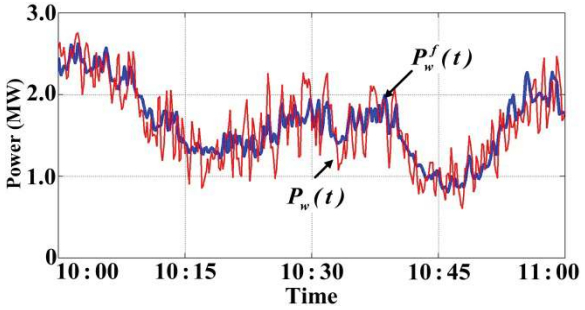

Fig. 13. Actual wind power and forecasted wind power.

ensure the hybrid system will dispatch stable power to satisfy the FMR under all wind conditions. Fig. 14 shows the system performance including the wind power, the dispatch power, the fluctuation level of the dispatch power, the SOC and power of ESS, and the power control signal $P_c(t)$ that are shown from top to bottom. The initial SOC of the ESS is set in the middle range (i.e. $SOC(0)=0.6$) which means the ESS energy status is in the normal condition at the beginning. Based on the fluctuation level of the dispatch power, we can see that the dispatch power fluctuation is maintained at less than 1% to meet the FMR. In addition, the proposed control algorithm is able to maintain the ESS power within 1.2MW of the power rating, while the SOC is maintained within a safe range from 0.2 to 1.0 as shown in Figs. 14(c) and 14(d), respectively. These performances verify the effectiveness of the proposed control algorithm. In order to obtain these performances, the proposed control algorithm adds the power control signal $P_c(t)$ according to the SOC of ESS. As shown in Fig. 14(e), because the SOC is in the normal condition at the beginning, it is not necessary to add the power control signal to the dispatch power (i.e. $P_c(t)=0$). From 15:00, when the SOC reaches the lower limit, the power control signal $P_c(t)$ is added to the dispatch power with a negative value to reduce the dispatch power, so the ESS is charged to prevent the SOC from being lower than the lower limit.

To evaluate the proposed control algorithm in the case that the ESS energy is critical low, the system is operated with the ESS where the initial SOC is only 20% at the beginning. The system performance in this case is shown in Fig. 15 including the wind power, the dispatch power, the fluctuation level of dispatch power, the SOC and power of ESS, and the power control signal $P_c(t)$ that are shown from top to bottom. In this case, because the system operates with a low battery energy condition at the beginning, the power control signal $P_c(t)$ is added to the dispatch power with a negative value to reduce the dispatch power, so the ESS is charged to prevent the SOC from being lower than the lower limit. Afterward, the ESS energy recovers to a normal status. According to Figs. 15(a) to 15(d), it can be seen that the dispatch power is stabilized successfully to meet the FMR, although the ESS

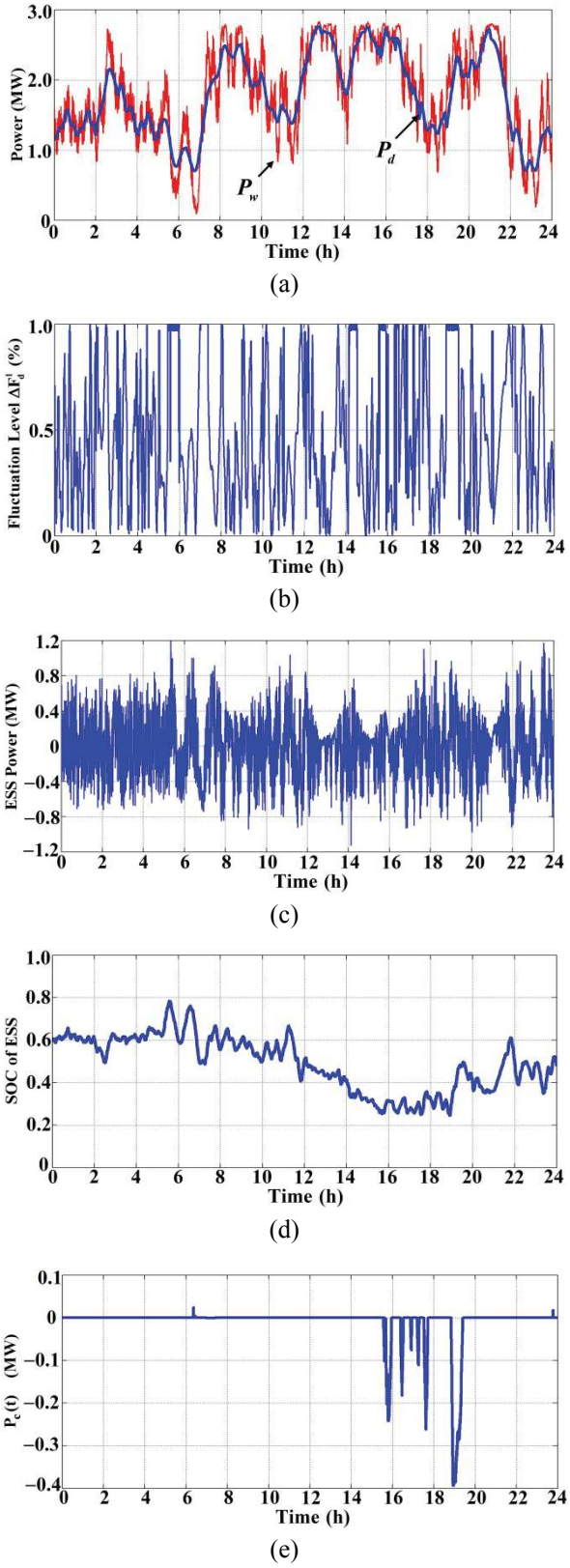

Fig. 14. Proposed control scheme performance in the short-term power dispatch. (a) Wind power and dispatch power. (b) Fluctuation level of dispatch power in 1-min. (c) ESS power. (d) SOC of ESS. (e) Control power signal $P_c(t)$.

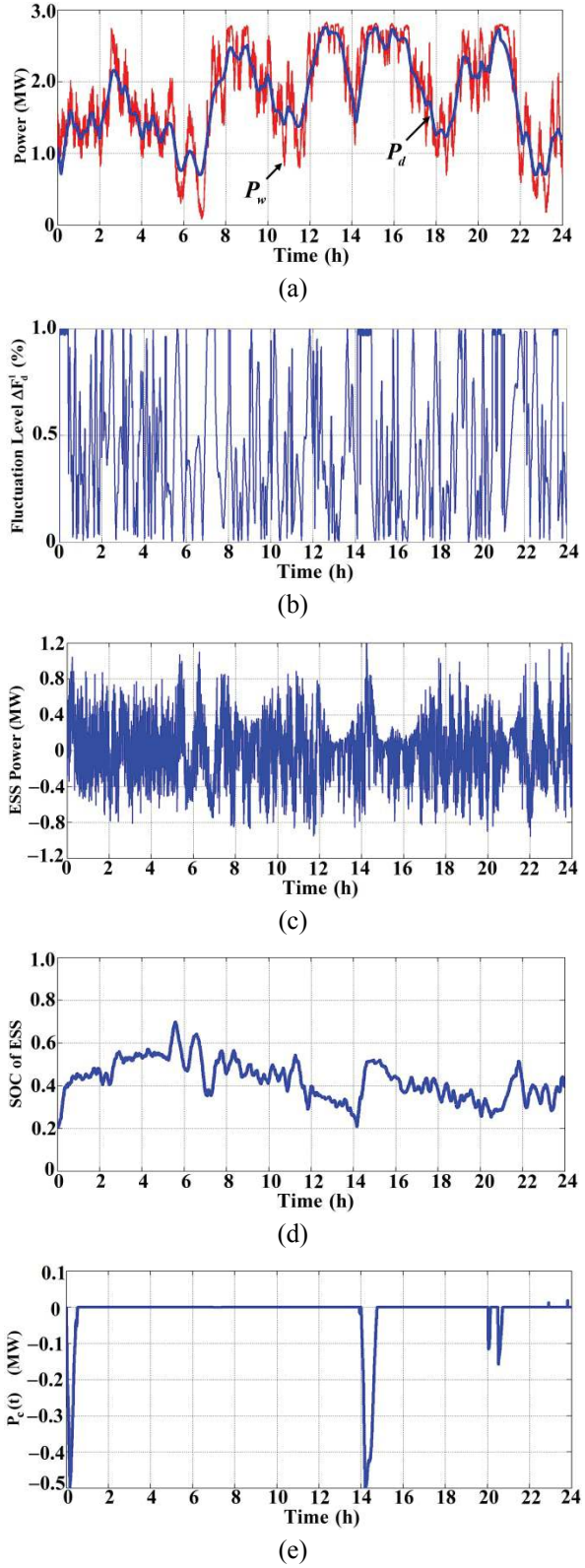

Fig. 15. Proposed control scheme performance in the short-term power dispatch when the ESS energy is empty at the beginning: (a) Wind power and dispatch power; (b) Fluctuation level of dispatch power in 1-min; (c) ESS power; (d) SOC of ESS; (e) Control power signal $P_c(t)$.

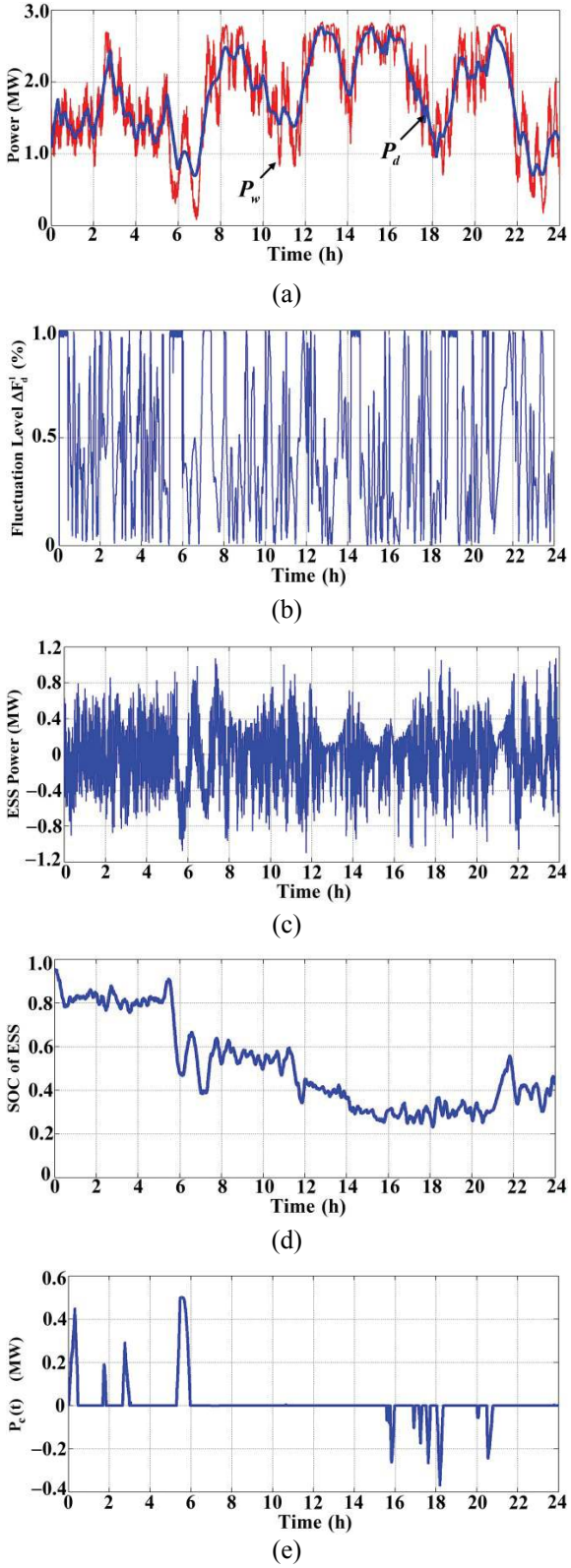

Fig. 16. Proposed control scheme performance in the short-term power dispatch when the ESS energy is full at the beginning: (a) Wind power and dispatch power; (b) Fluctuation level of dispatch power in 1-min; (c) ESS power; (d) SOC of ESS; (e) Control power signal $P_c(t)$.

energy is critically low at the beginning. In addition, the ESS power is regulated to be ower than the power rating during the system operation.

In Fig. 16, we evaluate the system performance when the ESS energy is almost full at the beginning. When the ESS energy is full, the positive value of the power control signal $P_c(t)$ is added to the dispatch power to increase the dispatch power, so the ESS is discharged to prevent the SOC from being higher than the upper limit. When the SOC descends to the normal condition, the power control signal $P_c(t)$ is zero, as shown in Fig. 16(e). From Figs. 15 and 16, the effectiveness of the proposed control algorithm is verified by features such as maintaining the ESS power to be lower than its rating, maintaining the SOC within a safe range, and ensuring the power dispatch satisfies the FMR.

7. Conclusion

In this paper, we proposed an optimal power flow control strategy which can minimize the required ESS capacity in wind power applications. The dispatch power is determined by using a zero-phase delay LPF, which removes the phase delay between the dispatch power and the wind power. Unlike the conventional methods, the dispatch power ensures the required FMR with the minimal ESS capacity by optimizing the filter time constant in each dispatching interval. Furthermore, a short-term power dispatch control algorithm is developed suitable for the proposed power dispatch with the zero-phase delay LPF, so that the SOC and the power of ESS are regulated effectively to be in the predefined ranges by adding a power control signal into the dispatch power command. To verify the effectiveness of the proposed method, we performed several numerical examples by using a 3-MW wind turbine with real wind speed data measured on Jeju Island. The results show that the proposed method minimizes the ESS capacity for all wind conditions; the system cost is significantly reduced by using the proposed method.

Acknowledgment

This work was supported by the National Research Foundation of Korea grant funded by the Korean Government (NRF-2015R1D1A1A09058166).

References

[1] C. L. Nguyen, H. H. Lee, and T. W. Chun, "Cost optimized battery capacity and short-term power dispatch control for wind farm," *IEEE Trans. Ind. Appl.,* vol. 51, no. 1, pp. 595-606, Jan./Feb. 2015.

[2] M. P. Akter, S. Mekhilef, N. M. L. Tan, and H. Akagi "Stability and performance investigations of model predictive controlled active-front-end (AFE) rectifiers for energy storage systems," *Journal of Power Electronics*, vol. 15, no. 1, pp. 202-215, Jan. 2015.

[3] C. Luo and B. T. Ooi, "Frequency deviation of thermal power plants due to wind farms," *IEEE Trans. Energy Convers.,* vol. 21, no. 3, pp.708-716, Sep. 2006.

[4] D. G. Francisco, S. Andreas, G. B. Oriol, and V. R. Roberto, "A review of energy storage technologies for wind power applications," *Renew. & Sustain. Energy Reviews*, vol. 16, no. 4, pp. 2154-2171, May 2012.

[5] X. Y. Wang, D. V. Mahinda, and S. S. Choi, "Determination of battery storage capacity in energy buffer for wind farm," *IEEE Trans. Energy Convers.,* vol. 23, no. 3, pp. 868-878, Sept. 2008.

[6] P. Poonpun and W. T Jewell, "Analysis of the cost per kilowatt hour to store electricity," *IEEE Trans. Energy Convers.,* vol. 23, no. 2, pp. 529-534, June 2008.

[7] X. Wang, M. Yue, E. Muljadi, and W. Gao "Probabilistic approach for power capacity specification of wind energy storage systems," *IEEE Trans. Ind. Appl.,* vol. 50, no. 2, pp.1215-1224, Mar./Apr. 2014.

[8] Q. Jiang and H. Wang, "Two-time-scale coordination control for a battery energy storage system to mitigate wind power fluctuations," *IEEE Trans. Energy Convers.,* vol. 28, no. 1, pp. 52-61, Mar. 2013.

[9] S. Teleke, M. E. Baran, S. Bhattacharya, and A. Q. Huang, "Optimal control of battery energy storage for wind farm dispatching," *IEEE Trans. Energy Convers.,* vol. 25, no. 3, pp. 787-794, Sept. 2010.

[10] Q. Li, S. S. Choi, Y. Yuan, and D. L. Yao, "On the determination of battery energy storage capacity and short-term power dispatch of a wind farm," *IEEE Trans. Sustain. Energy,* vol. 2, no. 2, pp. 148-158, Apr. 2011.

[11] C. L. Nguyen and H. H. Lee, "A comparative analysis among power dispatching control strategies for hybrid wind and energy storage system," in *Proc. 20th int. conf. electrical engineering, ICEE 2014,* pp. 489-494, Jun. 2014.

[12] Q. Jiang, Y. Gong, and H. Wang, "A battery energy storage system dual-layer control strategy for mitigating wind farm fluctuations," *IEEE Trans. Power Syst.,* vol. 28, no. 3, pp. 3263-3273, Aug. 2013.

[13] C. L. Nguyen and H. H. Lee, "Optimization of wind power dispatch to minimize energy storage system capacity," *Journal of Electrical Engineering & Technology*, vol. 9, no. 3, pp. 1080-1088, May 2014.

[14] C. L. Nguyen, and H. H. Lee, "An optimal power flow control strategy to minimize energy storage system capacity in wind power application," *The Int. Smart Grid Conf. (ISGC 2015),* Korea, pp.56-62, Oct. 2015.

[15] A. Uehara, A. Pratap, T. Goya, T. Senjyu, A. Yona, N. Urasaki, and T. Funabashi, "A coordinated control method to smooth wind power fluctuations of a PMSG-based WECS," *IEEE Trans. Energy Convers.*, vol. 26, no. 2, pp. 550-558, Feb. 2011.
[16] M. M. Chowdhury, M. E. Haque, M. Aktarujjaman, M. Negnevitsky, and A. Gargoom, "Grid integration impacts and energy storage systems for wind energy applications - A review," in *Proc. IEEE Power & Energy Society General Meeting,* pp. 1-8, Jul. 2011.
[17] M. Tsili and S. Papathanassiou, "A review of grid code technical requirements for wind farms," *IET Renew. Power Generation,* vol. 3, no. 3, pp. 308-332, Sept. 2009.
[18] X. Xi, R. Sioshansi, and V. Marano, "A stochastic dynamic programming model for co-optimization of distributed energy storage," *Energy Syst.,* vol. 5, no. 3, pp. 475-505, 2014.
[19] W. Wang, F. Wu, K. Zhao, L. Sun, J. Duan, and D. Sun, "Elimination of the state-of-charge errors for distributed battery energy storage devices in islanded droop-controlled microgrids", *Journal of Power Electronics*, vol. 15, no. 4, pp. 1105-1118, Jul. 2015.
[20] F. Luo, K. Meng, Z. Y. Dong, Y. Zheng, Y. Chen, and K. P. Wong, "Coordinated operational planning for wind farm with battery energy storage system," *IEEE Trans. Sustain. Energy,* vol. 6, no. 1, pp. 253-262, Jan. 2015.
[21] B. Hartmann and A. Dán, "Methodologies for storage size determination for the integration of wind power," *IEEE Trans. Sustain. Energy,* vol. 5, no. 1, pp. 182-189, Jan. 2014.
[22] D. L. Yao, S. S. Choi, K. J. Tseng, and T. T. Lie, "Determination of short-term power dispatch schedule for a wind farm incorporated with dual-battery energy storage scheme," *IEEE Trans. Sustain. Energy,* vol. 3, no. 1, pp. 74-84, Jan. 2012.
[23] S. Chai, Z. Xu, L. L. Lai, and K. P. Wong, "An overview on wind power forecasting methods," in *Proc. 2015 Int. Conf. on Machine Learning & Cybernetics,* pp.765-770, July 2015.
[24] J. Wang and F. Yang, "Optimal capacity allocation of standalone wind/ solar/battery hybrid power system based on improved particle swarm optimization algorithm," *IET Renewable Power Gener.,* vol. 7, no. 5, pp. 443-448, 2013.
[25] A. J. Pryde and R. M. Phatarfod, "Multiplicities of eigenvalues of some linear search schemes," *Linear Algebra Appl.,* vol. 291, no. 1, pp. 115-124, Apr. 1999.
[26] General Specification of Vestas V112-3.0 MW 50/60 Hz [Online]. Available: http://www.vestas.cz/files/V126-30.pdf

Cong-Long Nguyen received the B.S. degree in electrical engineering from the Ho Chi Minh City University of Technology, Ho Chi Minh City, Vietnam, in 2010, and the Ph.D. degree in electrical engineering from the University of Ulsan, Ulsan, South Korea, in 2016. He was with Intel Corporation as a Production Engineer to set up the CPU and chipset test systems at Intel Products Vietnam. He is currently a Postdoctoral Fellow with the Department of Electrical Engineering, École de technologie supérieure, University of Quebec, Canada. His research interests include applications of energy storage devices in renewable energy conversion systems, power electronics in electric vehicles, power quality control, dc and ac microgrids, and microbial fuel cells.

Hong-Hee Lee received his B.S., M.S., and Ph.D. degrees in Electrical Engineering from Seoul National University, Seoul, Korea, in 1980, 1982, and 1990, respectively. From 1994 to 1995, he was a Visiting Professor with Texas A&M University, College Station, TX, USA. Since 1985, he has been with the Department of Electrical Engineering, University of Ulsan, Ulsan, Korea, where he is currently a Professor in the School of Electrical Engineering. He is also the Director of the Network-based Automation Research Center, which is sponsored by the Ministry of Trade, Industry, and Energy. His research interests include power electronics, network-based motor control, and renewable energy. Dr. Lee is a member of the Institute of Electrical and Electronics Engineers (IEEE), the Korean Institute of Power Electronics (KIPE), the Korean Institute of Electrical Engineers (KIEE), and the Institute of Control, Robotics and Systems (ICROS). He was the President of KIPE in 2014.